

Analysis of the semileptonic decay

$$D^0 \rightarrow \bar{K}^0 \pi^- \mu^+ \nu$$

The FOCUS Collaboration ^{*}

J. M. Link ^a, P. M. Yager ^a, J. C. Anjos ^b, I. Bediaga ^b,
C. Göbel ^b, A. A. Machado ^b, J. Magnin ^b, A. Massafferri ^b,
J. M. de Miranda ^b, I. M. Pepe ^b, E. Polycarpo ^b,
A. C. dos Reis ^b, S. Carrillo ^c, E. Casimiro ^c, E. Cuautle ^c,
A. Sánchez-Hernández ^c, C. Uribe ^c, F. Vázquez ^c, L. Agostino ^d,
L. Cinquini ^d, J. P. Cumalat ^d, B. O'Reilly ^d, I. Segoni ^d,
K. Stenson ^d, J. N. Butler ^e, H. W. K. Cheung ^e, G. Chiadini ^e,
I. Gaines ^e, P. H. Garbincius ^e, L. A. Garren ^e, E. Gottschalk ^e,
P. H. Kasper ^e, A. E. Kreymer ^e, R. Kutschke ^e, M. Wang ^e,
L. Benussi ^f, M. Bertani ^f, S. Bianco ^f, F. L. Fabbri ^f, A. Zallo ^f,
M. Reyes ^g, C. Cawfield ^h, D. Y. Kim ^h, A. Rahimi ^h, J. Wiss ^h,
R. Gardner ⁱ, A. Kryemadhi ⁱ, Y. S. Chung ^j, J. S. Kang ^j,
B. R. Ko ^j, J. W. Kwak ^j, K. B. Lee ^j, K. Cho ^k, H. Park ^k,
G. Alimonti ^l, S. Barberis ^l, M. Boschini ^l, A. Cerutti ^l,
P. D'Angelo ^l, M. DiCorato ^l, P. Dini ^l, L. Edera ^l, S. Erba ^l,
P. Inzani ^l, F. Leveraro ^l, S. Malvezzi ^l, D. Menasce ^l,
M. Mezzadri ^l, L. Moroni ^l, D. Pedrini ^l, C. Pontoglio ^l,
F. Prezl ^l, M. Rovere ^l, S. Sala ^l, T. F. Davenport III ^m,
V. Arena ⁿ, G. Boca ⁿ, G. Bonomi ⁿ, G. Gianini ⁿ, G. Liguori ⁿ,
D. Lopes Pegna ⁿ, M. M. Merlo ⁿ, D. Pantea ⁿ, S. P. Ratti ⁿ,
C. Riccardi ⁿ, P. Vitulo ⁿ, H. Hernandez ^o, A. M. Lopez ^o,
H. Mendez ^o, A. Paris ^o, J. Quinones ^o, J. E. Ramirez ^o,
Y. Zhang ^o, J. R. Wilson ^p, T. Handler ^q, R. Mitchell ^q,
D. Engh ^r, M. Hosack ^r, W. E. Johns ^r, E. Luiggi ^r, J. E. Moore ^r,
M. Nehring ^r, P. D. Sheldon ^r, E. W. Vaandering ^r, M. Webster ^r,
M. Sheaff ^s

^a *University of California, Davis, CA 95616*

^b *Centro Brasileiro de Pesquisas Físicas, Rio de Janeiro, RJ, Brasil*

^{*} See <http://www-focus.fnal.gov/authors.html> for additional author information.

^c*CINVESTAV, 07000 México City, DF, Mexico*

^d*University of Colorado, Boulder, CO 80309*

^e*Fermi National Accelerator Laboratory, Batavia, IL 60510*

^f*Laboratori Nazionali di Frascati dell'INFN, Frascati, Italy I-00044*

^g*University of Guanajuato, 37150 Leon, Guanajuato, Mexico*

^h*University of Illinois, Urbana-Champaign, IL 61801*

ⁱ*Indiana University, Bloomington, IN 47405*

^j*Korea University, Seoul, Korea 136-701*

^k*Kyungpook National University, Taegu, Korea 702-701*

^l*INFN and University of Milano, Milano, Italy*

^m*University of North Carolina, Asheville, NC 28804*

ⁿ*Dipartimento di Fisica Nucleare e Teorica and INFN, Pavia, Italy*

^o*University of Puerto Rico, Mayaguez, PR 00681*

^p*University of South Carolina, Columbia, SC 29208*

^q*University of Tennessee, Knoxville, TN 37996*

^r*Vanderbilt University, Nashville, TN 37235*

^s*University of Wisconsin, Madison, WI 53706*

Abstract

Using data collected by the fixed target Fermilab experiment FOCUS, we present several first measurements for the semileptonic decay $D^0 \rightarrow \bar{K}^0 \pi^- \mu^+ \nu$. Using a model that includes a $\bar{K}^0 \pi^-$ S-wave component, we measure the form factor ratios to be $r_v = 1.706 \pm 0.677 \pm 0.342$ and $r_2 = 0.912 \pm 0.370 \pm 0.104$ and the S-wave amplitude to be $A = 0.347 \pm 0.222 \pm 0.053 \text{ GeV}^{-1}$. Finally, we measure the vector semileptonic branching ratio $\frac{\Gamma(D^0 \rightarrow K^{*(892)-} \mu^+ \nu)}{\Gamma(D^0 \rightarrow \bar{K}^0 \pi^- \pi^+)} = 0.337 \pm 0.034 \pm 0.013$.

1 Introduction

Cabibbo allowed semileptonic decays have relatively large branching fractions and can be easily selected to achieve low levels of background contamination. The experimental results can be directly compared to theory where decay rates are calculated from first principles and include QCD effects in the form factors. Form factors are predicted in several models (quark models [1], Lattice QCD [2], and sum rules [3]). Once the form factors are determined, the CKM matrix elements can be calculated. While there have been several measurements of the D^+ [4,5,6,7,8,9] form factors, there are still no measurements

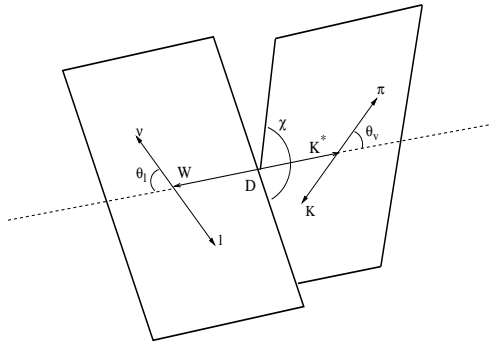


Fig. 1. Schematic of the decay $D \rightarrow K^* \ell^+ \nu$ for angular variables definition.

of the D^0 form factors for the vector semileptonic decays. We present the first measurement of the D^0 semileptonic form factor ratios for vector channels and the branching ratio $\Gamma(D^0 \rightarrow K^*(892)^- \mu^+ \nu) / \Gamma(D^0 \rightarrow \bar{K}^0 \pi^- \pi^+)$.¹ Furthermore, we present an investigation of the S-wave component of the $\bar{K}^0 \pi^-$ system and the measurement of its amplitude. This S-wave representation [10] was first used by FOCUS for the analysis of the decay $D^+ \rightarrow K^- \pi^+ \mu^+ \nu$.

The four-body decay amplitude can be parameterized by two masses and three angles. We use $M(\bar{K}^0 \pi^-)$, $q^2 = (P_\mu + P_\nu)^2$, and the three angles defined in Fig. 1: $\cos \theta_V$ (the angle between the π and the D in the K^* rest frame), $\cos \theta_\ell$ (the angle between the ν and the D in the W rest frame), and χ (the angle between the decay planes of the K^* and the W).

With these definitions the decay amplitude is written as:²

$$\frac{d^5 \Gamma}{dm_{K\pi} dq^2 d \cos \theta_v d \cos \theta_\ell d \chi} \propto K(q^2 - m_\ell^2) \quad (1)$$

$$\left\{ \begin{array}{l} \left| \begin{array}{l} (1 + \cos \theta_\ell) \sin \theta_v e^{i\chi} B_{K^*-} H_+ \\ -(1 - \cos \theta_\ell) \sin \theta_v e^{-i\chi} B_{K^*-} H_- \\ -2 \sin \theta_\ell (\cos \theta_v B_{K^*-} + A e^{i\delta}) H_0 \end{array} \right|^2 \\ + \frac{m_\ell^2}{q^2} \left| \begin{array}{l} \sin \theta_\ell \sin \theta_v B_{K^*-} (e^{i\chi} H_+ + e^{-i\chi} H_-) \\ + 2 \cos \theta_\ell (\cos \theta_v B_{K^*-} + A e^{i\delta}) H_0 \\ + 2 (\cos \theta_v B_{K^*-} + A e^{i\delta}) H_t \end{array} \right|^2 \end{array} \right\}$$

where K is the $K\pi$ system momentum in the D rest frame and B_{K^*-} and $A e^{i\delta}$ are the Breit-Wigner and the S-wave components describing the spin one and

¹ Charge conjugation is implied throughout this letter.

² This model assumes that the q^2 dependence of the S-wave amplitude coupling to the virtual W^+ is the same as the H_0 helicity amplitude describing the K^* component. A study with as much as 100 times the statistics of this analysis has been performed for the FOCUS analysis of the decay $D^+ \rightarrow K^- \pi^+ \mu^+ \nu$ [10]. This study, where a significantly different kinematic dependence for the S-wave has been used, has reported a change in the form factors of less than 6% of the statistical error.

spin zero states of $\bar{K}^0\pi^-$, respectively. The four form factors ($A_{1,2,3}$ and V) that are necessary to describe a decay $D \rightarrow V\ell\nu$ (where V stands for Vector), are included in the four helicity amplitudes:

$$H_{\pm}(q^2) = [(M_D + m_{K\pi})A_1(q^2) \mp \frac{2M_D K}{M_D + m_{K\pi}}V(q^2)] \quad (2)$$

$$H_0(q^2) = \frac{1}{2m_{K\pi}\sqrt{q^2}}[(M_D^2 - m_{K\pi}^2 - q^2)(M_D + m_{K\pi})A_1(q^2) - \frac{4M_D^2 K^2}{M_D + m_{K\pi}}A_2(q^2)] \quad (3)$$

$$H_t(q^2) = \frac{M_D K}{m_{K\pi}\sqrt{q^2}}[(M_D + m_{K\pi})A_1(q^2) - \frac{M_D^2 - m_{K\pi}^2 + q^2}{M_D + m_{K\pi}}A_2(q^2) + \frac{2q^2}{M_D + m_{K\pi}}A_3(q^2)] \quad (4)$$

A pole mass form is assumed for the form factors:

$$A_i(q^2) = \frac{A_i(0)}{1 - \frac{q^2}{M_A^2}} \quad V(q^2) = \frac{V(0)}{1 - \frac{q^2}{M_V^2}} \quad (5)$$

where M_A and M_V are the masses of the lowest $c\bar{s}$ states with the same quantum numbers as the W , namely $M_A = 2.5 \text{ GeV}/c^2$ and $M_V = 2.1 \text{ GeV}/c^2$ (which correspond to the masses of the D_{s1}^+ and D_s^{*+} , respectively). By including the parameter $A_1(0)$ in the constant that multiplies Eq. 1, the decay amplitude can be parameterized by the ratios of the form factors at $q^2 = 0$:

$$r_v = \frac{V(0)}{A_1(0)}, \quad r_2 = \frac{A_2(0)}{A_1(0)}, \quad r_3 = \frac{A_3(0)}{A_1(0)} \quad (6)$$

We measure r_v and r_2 . We have inadequate sensitivity to determine r_3 and we set its value to zero. From variations of this value we determine that the systematic uncertainty from setting $r_3 = 0$ is negligible.

2 Event Reconstruction and Selection

FOCUS is a photoproduction experiment which collected data during the 1996–1997 fixed-target run at Fermilab. The experiment, which is an upgrade of Fermilab experiment E687 [11,12], is characterized by excellent vertex resolution and particle identification. For about 2/3 of the data taking the experimental target was interleaved with a target silicon system [13]. The track

reconstruction downstream of the target is performed by four stations of silicon microstrips (SSD) and five stations of proportional wire chambers. The momentum of charged tracks is measured by the deflection in two magnets of opposite polarity. Charged particle identification is performed by three multi-cell threshold Čerenkov counters for electrons, pions, kaons, and protons [14]. Combining the information on the track momentum and the number of photoelectrons produced in the cells inside the $\beta = 1$ cone, a negative log-likelihood variable (W) for the hypothesis of the particle to be an electron, pion, kaon, or proton is determined. Particle identification is performed by a comparison of the probabilities for the different hypotheses and by requiring the hypothesis for the candidate particle to be higher than for the other hypotheses. Muons are identified by the hits left in tracking systems after penetrating approximately 21 interaction lengths of shielding material [10].

In reconstructing $D^0 \rightarrow \bar{K}^0 \pi^- \mu^+ \nu$, we select combinations of two charged tracks of opposite sign where one is identified as a pion and the other as a muon. For pion identification we require the pion hypothesis not to be disfavored by more than six units of log-likelihood compared to the hypothesis with highest confidence level ($\min(W) - W_\pi > -6$), and to be favored by one unit of log-likelihood over the kaon hypothesis (to reduce the contamination from $D^0 \rightarrow K^- \mu^+ \nu$). For muon identification we require the track to have been reconstructed in the muon system (with at most one plane missed) with a confidence level greater than 1%. In order to reject background from the decays $\pi^+ / K^+ \rightarrow \mu^+ \nu$, we require the muon trajectory to be consistent through the two analysis magnets with a confidence level greater than 1%. Each track must have momentum greater than 10 GeV/ c .

The two tracks are used to form the D^0 decay vertex, which is required to have C.L. > 5%, where C.L. is the confidence level. To reduce contamination from higher multiplicity decays, we require the probability for any other track reconstructed in the SSD system to come from the decay vertex to be lower than 0.1%. This requirement does not apply to the tracks used for the primary vertex reconstruction. To minimize background from hadronic re-interactions in the target, the decay vertex must lie at least one sigma outside of the target. The \bar{K}^0 is reconstructed as a K_S^0 from the decay $K_S^0 \rightarrow \pi^- \pi^+$ [15]. The invariant mass is required to be within three sigma of the nominal K_S^0 mass. If the pions are reconstructed using information from the silicon vertex detectors, the reconstructed K_S^0 direction is used in the reconstruction of the D^0 vertex. In order to enhance the probability that our $K_S^0 \pi^-$ combination comes from a $K^*(892)^-$, we require the reconstructed $K_S^0 \pi^-$ mass to be within one Γ of the nominal $K^*(892)^-$ mass. The $K^*(892)^-$ natural width Γ (50 MeV/ c^2) is much larger than the experimental resolution on the reconstructed $K_S^0 \pi^-$ mass (5 MeV/ c^2). The invariant mass $M(K_S^0 \pi^- \mu^+)$ is required to be lower than 1.8 GeV/ c^2 . This cut significantly reduces combinatoric background since $M(K_S^0 \pi^- \mu^+)$ is kinematically limited to be below the nominal D^0 mass and

rejects $D^0 \rightarrow K_S^0 \pi^- \pi^+$ decays when one of the pions is misidentified as a muon.

We use the SSD tracks which have not been used in the D^0 decay reconstruction to form primary vertex candidates. Each candidate is formed by starting with two tracks that make a vertex with C.L. > 1% and adding other tracks so long as the C.L. remains greater than 1%. When a vertex is formed the remaining tracks are used to form a second candidate in the same way and so on for the other candidates. We select the candidate with the highest multiplicity, and arbitrate ties by keeping the one with higher significance of separation from the secondary vertex. The significance of separation, which is given by the ratio of the distance between the two vertices divided by its error (ℓ/σ_ℓ), is required to satisfy $\ell/\sigma_\ell > 5$. We “tag” the D^0 by requiring that it comes from the decay $D^{*+} \rightarrow D^0 \pi_s^+$. The kinematics of this decay result in the pion having low momentum and being called a “slow” pion (π_s). The pion must be one of the tracks used in the primary vertex reconstruction. It must have $\min(W) - W_\pi > -6$ and $p > 2$ GeV/c.

3 Fitting for the Form Factor Ratios and $\overline{K}^0 \pi^-$ S-wave Amplitude

In order to determine the form factor ratios r_v and r_2 we use a combined fit of the mass difference $\Delta M = M(D^*) - M(D)$ and the three dimensional distribution $\cos \theta_V$ vs. $\cos \theta_\ell$ vs. q^2 . For the ΔM component we use 60 bins in the region 0.14–0.20 GeV/c². For the $\cos \theta_V$ vs. $\cos \theta_\ell$ vs. q^2 distribution we select events with $\Delta M < 0.15$ GeV/c², and divide the phase space into four equally spaced bins for each of the two angular variables and two equally spaced bins for q^2 . The ΔM distribution, where signal and background events have a very different shape, is used to evaluate the background level. The binning choice for $\cos \theta_V$ vs. $\cos \theta_\ell$ vs. q^2 gives information on the angular distributions of the W and the $\overline{K}^0 \pi^-$ decays for two regions of q^2 . At low q^2 the angular dependence is more dramatic, while a more isotropic behavior is expected for high q^2 values, where the helicity amplitudes contribute with similar strength.

Two methods are used to find the momentum of the missing neutrino. To compute the q^2 we use a “ D^* cone” algorithm. By imposing energy and momentum conservation in the $K^* \mu$ rest frame and by constraining the D and the D^* to their nominal masses, the magnitude of $p(D^0)$ (which in this frame is equal to $p(\nu)$) is determined, but the direction lies on a cone. The direction is chosen by selecting the solution that gives the best χ^2 when compared to the D^0 direction as given by the line connecting the two vertices. To compute the mass difference, we determine the neutrino momentum using the “neutrino closure” algorithm. This method is based on energy and momentum conservation for

the decay $D^0 \rightarrow \overline{K}^0 \pi^- \mu^+ \nu$ and uses the nominal mass of the D^0 meson. The algorithm allows us to determine the neutrino momentum up to a two fold ambiguity, which is resolved by choosing the solution with lowest ΔM . Monte Carlo studies show that this choice is most often the correct solution.

We use a binned maximum likelihood fitting technique with:

$$\mathcal{L} = \prod_{ijk} \frac{n_{ijk}^{s_{ijk}} e^{-n_{ijk}}}{s_{ijk}!} \times \prod_m \frac{N_m^{S_m} e^{-N_m}}{S_m!} \quad (7)$$

where s_{ijk} (n_{ijk}) is the number of observed (expected) events in the ijk^{th} bin of the three dimensional distribution and S_m (N_m) is the number of observed (expected) events in the ΔM distribution. The number of expected events is given by signal and background contributions. Non-charm backgrounds are essentially removed by the ℓ/σ_ℓ requirement, by discarding events where the reconstructed decay vertex of the D^0 lies within one standard deviation from the target, and by the muon requirement. Contamination from charm decays is accounted for by using a Monte Carlo (that will be called MC_{BKG}) which simulates all known charm decays other than our signal mode. The shapes for both distributions are taken from the distributions of the reconstructed events in MC_{BKG}, and their amplitudes are free to float. The background levels in the two distributions are tied by imposing that the yield of the MC_{BKG} in the $\cos \theta_V$ vs. $\cos \theta_\ell$ vs. q^2 distribution is equal to the area of the background shape in the ΔM distribution for $\Delta M < 0.15 \text{ GeV}/c^2$. This corresponds to the selection cut imposed on the events in the $\cos \theta_V$ vs. $\cos \theta_\ell$ vs. q^2 distribution. For the ΔM distribution, the signal shape is taken from Monte Carlo generated $D^0 \rightarrow \overline{K}^0 \pi^- \mu^+ \nu$ events. For $\cos \theta_V$ vs. $\cos \theta_\ell$ vs. q^2 the signal contribution to n_{ijk} is computed as the number of events generated in the bin ijk corrected by the efficiency for that bin. We calculate the generated number of event in bin ijk as a function of the fit parameters r_v and r_2 using a Monte Carlo event weighting procedure based on Ref. [16]. For each Monte Carlo event generated in the bin ijk , we fill that bin with a weight given by the ratio of the decay amplitude in Eq. 1 evaluated for the fit parameters r_v and r_2 over the decay amplitude evaluated for the input Monte Carlo values.³ The signal yields in the $\cos \theta_V$ vs. $\cos \theta_\ell$ vs. q^2 and in the ΔM distributions are constrained in the same way as explained for the background events.

The combined fit is shown in Fig. 2. The number of signal events is 175 ± 17 . The χ^2 per degree of freedom in Fig. 2b is 32/27 which corresponds to a

³ The FOCUS Monte Carlo simulation uses the $D^+ \rightarrow K^- \pi^+ \mu^+ \nu$ form factor ratios and the S-wave parameters measured in [4]: $r_v = 1.504 \pm 0.057 \pm 0.039$, $r_2 = 0.875 \pm 0.049 \pm 0.064$, $A = 0.330 \pm 0.022 \pm 0.015$, and $\delta = 0.68 \pm 0.07 \pm 0.05$.

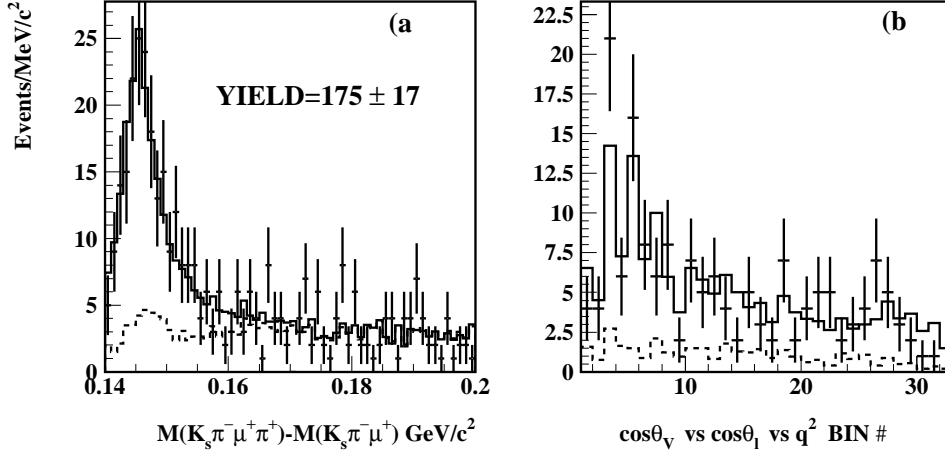


Fig. 2. a) ΔM fit, b) $\cos \theta_V$ vs. $\cos \theta_\ell$ vs. q^2 fit. Points with error bars are data, histogram is the fit, dashed line is the background component.

confidence level of 22%. We measure the form factor ratios to be:

$$r_v = 1.706 \pm 0.677 \quad (8)$$

$$r_2 = 0.912 \pm 0.370 \quad (9)$$

where the errors are statistical.

The fit for the amplitude of the S-wave is performed with the same technique as the fit for the form factor ratios. We fix the form factor ratios to the values found above and, based on isospin symmetry, we fix the phase to 0.68, the value measured for the $D^+ \rightarrow K^- \pi^+ \mu^+ \nu$ decay. As described in section 5, the possible bias due to this assumption is included in the systematic uncertainty evaluation. We find that A does not depend strongly on the phase. We measure:

$$A = 0.347 \pm 0.222 \text{ GeV}^{-1} \quad (10)$$

where the error is statistical.

4 The Branching Ratio $\Gamma(D^0 \rightarrow K^*(892)^- \mu^+ \nu) / \Gamma(D^0 \rightarrow \bar{K}^0 \pi^- \pi^+)$

The branching ratio is measured by dividing the efficiency corrected yields of the two modes. The normalization mode $D^0 \rightarrow \bar{K}^0 \pi^- \pi^+$ is reconstructed following the same procedure and applying the same requirements as for the

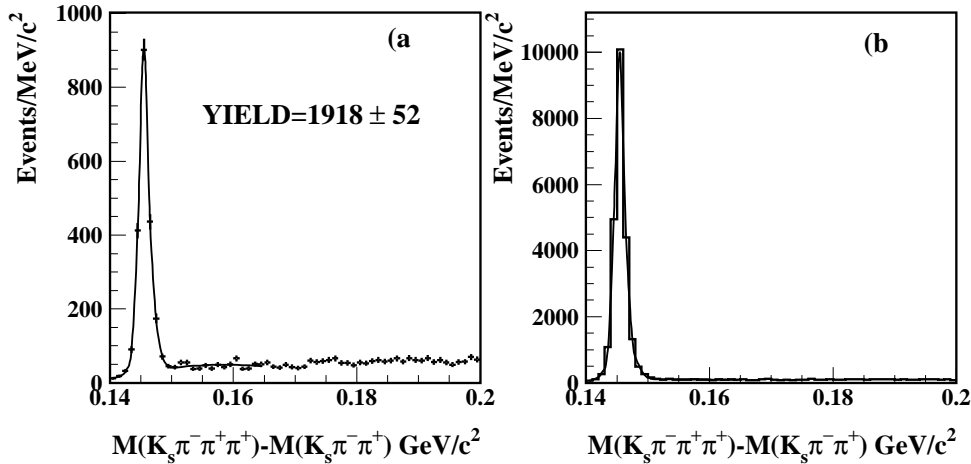


Fig. 3. ΔM fit for data (a) and Monte Carlo (b). The signal is fit to two Gaussian distributions, the background is fit to the threshold function in Eq. 11.

$D^0 \rightarrow \bar{K}^0 \pi^- \mu^+ \nu$ mode (when possible), in order to minimize bias due to possible inaccuracies in the Monte Carlo evaluation of the efficiency for the K_S^0 , which is reconstructed in a very different way from ordinary tracks. D^{*+} tag, vertex reconstruction, K_S^0 reconstruction, and particle identification (except muon identification) are the same as for the semileptonic mode. The π with the opposite charge of the π_s must pass identical requirements as the π^- in the semileptonic mode. The trajectory of the π with the same charge as the π_s must be consistent through the two analysis magnets, as we require for the μ^+ . In addition it is required to have $\min(W) - W_\pi > -6$. For the hadronic mode we do not require the event to be in the mass window around the $K^*(892)^-$ nominal mass. The invariant mass $M(K_S^0 \pi^- \pi^+)$ must lie within $24 \text{ MeV}/c^2$ of the fit D^0 mass, both for data and Monte Carlo. This window corresponds to a two sigma cut. The ΔM distribution is fit to two Gaussian distributions for the signal (in order to account for different resolutions) and the following threshold function for the background:

$$\text{BKG}(\Delta M) = a (\Delta M - m_\pi)^{1/2} + b (\Delta M - m_\pi)^{3/2} + c (\Delta M - m_\pi)^{5/2} \quad (11)$$

The fit for data and Monte Carlo are shown in Fig. 3. The yield from the fit to the data is 1918 ± 52 events.

The efficiency corrected yield of $D^0 \rightarrow K^*(892)^- \mu^+ \nu$ is determined by correcting the efficiency corrected yield of $D^0 \rightarrow \bar{K}^0 \pi^- \mu^+ \nu$ for the amount of K^{*-} in the $\bar{K}^0 \pi^-$ system. Since the Monte Carlo simulation uses the form factor ratios and S-wave parameters measured in the much higher statistics FOCUS analysis of $D^+ \rightarrow K^- \pi^+ \mu^- \nu$, which are in excellent agreement with that mea-

sured in the present analysis, we estimate that the correction factors for the number of reconstructed events in data and Monte Carlo are the same, and therefore cancel out. The number of generated events in Monte Carlo (which is used to calculate the efficiency) must be corrected by the relative branching ratio $\Gamma(D^0 \rightarrow K^*(892)^-\mu^+\nu)/\Gamma(D^0 \rightarrow \bar{K}^0\pi^-\mu^+\nu)$ used for the Monte Carlo simulation. This can be evaluated by integrating over phase space the decay amplitude when the exclusive K^* mode is generated, and dividing by the integral over phase space of the decay amplitude for the inclusive mode. We calculate that in our Monte Carlo simulation the branching ratio is 0.95. We measure the branching ratio to be:

$$\frac{\Gamma(D^0 \rightarrow K^*(892)^-\mu^+\nu)}{\Gamma(D^0 \rightarrow \bar{K}^0\pi^-\mu^+\nu)} = 0.337 \pm 0.034 \quad (12)$$

where the error is statistical.

5 Systematic Uncertainty Evaluation

We carefully considered and evaluated many possible sources of systematic uncertainty in our results. Systematic bias can be generated by a poor Monte Carlo simulation of the detector performance, resulting in erroneous estimation of the efficiency. Also the particular choice for the fitting technique and parameters may bias the measurement.

The accuracy and correct estimation of the errors reported by the fitting method is evaluated by repeating the measurement on a thousand samples obtained from fluctuating the bin entries in the data histogram. From the Gaussian distribution of the returned values for each measured quantity (form factor ratios, S-wave amplitude, signal and background yields), we conclude that the fit method is not affected by systematic bias and returns correct values for the errors.

The Monte Carlo evaluation of the efficiency is investigated by repeating the measurements for different variations of the selection cuts. As expected, when the efficiency is correctly estimated (for our level of accuracy), the results are always stable within errors. We evaluate a possible bias due to the Monte Carlo simulation with the “split sample” technique, derived from the S-factor method used by the Particle Data Group [17]. The data is split into statistically independent samples; for example, if the momentum simulation is being investigated, the data is split into distinct momentum regions. The measurement is performed on each sample for the observable x (e.g. r_v) and a χ^2 for the hypothesis that the independent measurements are consistent is calculated. A poor consistency might result from a badly estimated efficiency with respect

to the momentum. We define poor consistency to be the case where $\chi^2 > 1$. In this case, the errors on the different measurements are scaled in order to return $\chi^2 = 1$, and we calculate a systematic uncertainty for the x measurement by subtracting in quadrature the statistical error from the scaled error on the weighted average of the independent measurements. Additional details are given in Ref. [18].

The bias from fitting choices is evaluated as the variance of measurements obtained by varying such choices. We vary the bin size both for the ΔM and the $\cos \theta_V$ vs. $\cos \theta_\ell$ vs. q^2 distributions. For ΔM , we also vary the fitting range. The r_v and r_2 parameters are also evaluated setting the S-wave parameters to zero. The S-wave amplitude is evaluated for two additional values of the phase (at plus and minus one sigma from the reference value). For the r_v , r_2 , and A fits, we include a variation on the fitting technique. This second fitting technique accounts for the efficiency in a different way. The efficiency is taken into account by using the weighting method on the reconstructed Monte Carlo events, instead of the generated events. For each event that passes all the selection cuts, the bin in which the event was generated in is filled with the weight described in Section 3.

For the branching ratio measurement, we investigate the bias due to Monte Carlo input parameters by varying the form factor ratios and the S-wave values, and by varying the resonant structure of $\overline{K}^0 \pi^- \pi^+$. Also, a less refined simulation of the hadronic trigger is investigated. The systematic bias from the model used in the Monte Carlo is evaluated as the variance of the three measurements found with these variations and the standard result.

The total systematic uncertainty is given by the sum in quadrature of the uncertainties from the independent sources. Table 1 summarizes the results of the systematic uncertainty evaluation for all of the measurements. Including the systematic uncertainty we measure:

$$r_v = 1.706 \pm 0.677 \text{ (stat)} \pm 0.342 \text{ (sys)} \quad (13)$$

$$r_2 = 0.912 \pm 0.370 \text{ (stat)} \pm 0.104 \text{ (sys)} \quad (14)$$

$$A = 0.347 \pm 0.222 \text{ (stat)} \pm 0.053 \text{ (sys)} \text{ GeV}^{-1} \quad (15)$$

$$\frac{\Gamma(D^0 \rightarrow K^*(892)^- \mu^+ \nu)}{\Gamma(D^0 \rightarrow \overline{K}^0 \pi^- \pi^+)} = 0.337 \pm 0.034 \text{ (stat)} \pm 0.013 \text{ (sys)} \quad (16)$$

6 Conclusions

We have presented an analysis of the semileptonic decay $D^0 \rightarrow \overline{K}^0 \pi^- \mu^+ \nu$ using FOCUS data. Using a model which includes a $\overline{K}^0 \pi^-$ S-wave compo-

Table 1

The systematic uncertainties from the Monte Carlo efficiency and acceptance evaluation, the fitting condition, and total for r_v , r_2 , A , and the branching ratio are shown. For the branching ratio, the systematic from the input parameters and trigger simulation in the Monte Carlo is also evaluated.

Systematic Error				
Source	$\sigma(r_v)$	$\sigma(r_2)$	$\sigma(A)(\text{GeV}^{-1})$	$\sigma(\text{BR})$
MC Simulation	0.0	0.0	0.0	0.0
Fit	0.342	0.104	0.053	0.002
Model	–	–	–	0.013
Total	0.342	0.104	0.053	0.013

ment that interferes with the dominant $K^*(892)^-$ state, we have measured for the first time the D^0 form factor ratios for vector channels and the S-wave amplitude. We also report the first measurement of the branching ratio $\Gamma(D^0 \rightarrow K^*(892)^-\mu^+\nu)/\Gamma(D^0 \rightarrow \bar{K}^0\pi^-\pi^+)$.

Table 2

The measurement of r_v , r_2 , and A presented in this letter are compared to the FOCUS results for the decay $D^+ \rightarrow K^-\pi^+\mu^+\nu$. We fix the S-wave phase to 0.68, the value measured for the D^+ .

	$D^0 \rightarrow \bar{K}^0\pi^-\mu^+\nu$	$D^+ \rightarrow K^-\pi^+\mu^+\nu$
r_v	$1.706 \pm 0.677 \pm 0.342$	$1.504 \pm 0.057 \pm 0.039$
r_2	$0.912 \pm 0.370 \pm 0.104$	$0.875 \pm 0.049 \pm 0.064$
$A(\text{GeV}^{-1})$	$0.347 \pm 0.222 \pm 0.053$	$0.330 \pm 0.022 \pm 0.015$

From isospin symmetry, the expected values of r_v , r_2 , and A can be directly compared to the results of the FOCUS measurements for the decay $D^+ \rightarrow K^-\pi^+\mu^+\nu$, which uses the same model as the analysis presented in this letter. We find excellent agreement with the values for the D^+ , see Table 2. We calculate that in our model, where the $\bar{K}^0\pi^-$ system is given by a scalar and a vector component, the scalar fraction is 6%.

The branching ratio value can also be estimated from the D^+ analysis using isospin symmetry:

$$\frac{\Gamma(D^0 \rightarrow K^{*-}\mu^+\nu)}{\Gamma(D^0 \rightarrow \bar{K}^0\pi^-\pi^+)} = \frac{\tau(D^0)}{\tau(D^+)} \times \frac{\Gamma(D^+ \rightarrow K^{*0}\mu^+\nu)}{\Gamma(D^+ \rightarrow K^-\pi^+\pi^+)} \times \frac{\mathcal{B}(D^+ \rightarrow K^-\pi^+\pi^+)}{\mathcal{B}(D^0 \rightarrow \bar{K}^0\pi^-\pi^+)} \quad (17)$$

Since the decay dynamics do not depend on the lepton species, we compare the

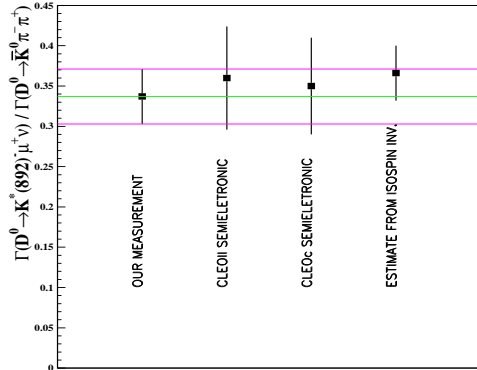


Fig. 4. The $\Gamma(D^0 \rightarrow K^*(892)^-\mu^+\nu)/\Gamma(D^0 \rightarrow \bar{K}^0\pi^-\pi^+)$ FOCUS measurement is compared to the CLEO-II measurement of the semielecronic mode $\Gamma(D^0 \rightarrow K^*(892)^-e^+\nu)/\Gamma(D^0 \rightarrow \bar{K}^0\pi^-\pi^+)$, with the CLEO-c preliminary measurement of $\mathcal{B}(D^0 \rightarrow K^*(892)^-e^+\nu_e)$ divided by the Particle Data Group average for $\mathcal{B}(D^0 \rightarrow \bar{K}^0\pi^-\pi^+)$, and to an estimate from isospin symmetry. The semielecronic results are corrected to account for the smaller electron mass when compared to the muon and they do not include the S-wave component.

branching ratio result to measurements that use the semielecronic channel. Differences in the decay rate are only due to the larger mass of the muon as compared to the electron. In the semimuonic mode the phase space is reduced and there is a more significant contribution from the m^2 term of the decay amplitude (see Eq. 1). According to the PDG, the electron values should be corrected by a factor of 0.952 to compare to the muon results. We apply this correction and compare our results to the CLEO-II measurement of $\Gamma(D^0 \rightarrow K^{*-}e^+\nu)/\Gamma(D^0 \rightarrow \bar{K}^0\pi^-\pi^+)$ [19]. We also compare our results to the recent preliminary result from CLEO-c of the absolute branching fraction $\mathcal{B}(D^0 \rightarrow K^{*-}e^+\nu)$ (presented in conference proceedings [20]) divided by the PDG average of $\mathcal{B}(D^0 \rightarrow \bar{K}^0\pi^-\pi^+)$. The comparison of our branching ratio measurement with the semielecronic results and with the calculation in Eq. 17 is shown in Fig. 4. Only the calculation from isospin symmetry includes the effects of the S-wave component. The three estimates come from different measurements, and are in excellent agreement with each other and with our measurement.

7 Acknowledgements

We wish to acknowledge the assistance of the staffs of Fermi National Accelerator Laboratory, the INFN of Italy, and the physics departments of the collaborating institutions. This research was supported in part by the U. S. National Science Foundation, the U. S. Department of Energy, the Italian Isti-

tuto Nazionale di Fisica Nucleare and Ministero dell'Università e della Ricerca Scientifica e Tecnologica, the Brazilian Conselho Nacional de Desenvolvimento Científico e Tecnológico, CONACyT-México, the Korean Ministry of Education, and the Korean Science and Engineering Foundation.

References

- [1] D. Scora and N. Isgur, *Phys. Rev. D* **52** (1995) 2783.
- [2] K. C. Bowler *et al.* [UKQCD Collaboration], *Phys. Rev. D* **52** (1995) 5067.
- [3] P. Ball, V. M. Braun and H. G. Dosch, *Phys. Rev. D* **44** (1991) 3567.
- [4] J. M. Link *et al.* [FOCUS Collaboration], *Phys. Lett. B* **544** (2002) 89.
- [5] M. Adamovich *et al.* [BEATRICE Collaboration], *Eur. Phys. J. C* **6** (1999) 35.
- [6] E. M. Aitala *et al.* [E791 Collaboration], *Phys. Rev. Lett.* **80** (1998) 1393.
- [7] E. M. Aitala *et al.* [E791 Collaboration], *Phys. Lett. B* **450** (1999) 294.
- [8] P. L. Frabetti *et al.* [E687 Collaboration], *Phys. Lett. B* **307** (1993) 262.
- [9] K. Kodama *et al.* [E653 Collaboration], *Phys. Lett. B* **274** (1992) 246.
- [10] J. M. Link *et al.* [FOCUS Collaboration], *Phys. Lett. B* **535** (2002) 43.
- [11] P. L. Frabetti *et al.* [E687 Collaboration], *Nucl. Instrum. Meth. A* **320** (1992) 519.
- [12] P. L. Frabetti *et al.* [E687 Collaboration], *Nucl. Instrum. Meth. A* **329** (1993) 62.
- [13] J. M. Link *et al.* [FOCUS Collaboration], *Nucl. Instrum. Meth. A* **516** (2004) 364.
- [14] J. M. Link *et al.* [FOCUS Collaboration], *Nucl. Instrum. Meth. A* **484** (2002) 270.
- [15] J. M. Link *et al.* [FOCUS Collaboration], *Nucl. Instrum. Meth. A* **484** (2002) 174.
- [16] D. M. Schmidt, R. J. Morrison and M. S. Witherell, *Nucl. Instrum. Meth. A* **328** (1993) 547.
- [17] S. Eidelman *et al.* [Particle Data Group], *Phys. Lett. B* **592** (2004) 1.
- [18] J. M. Link *et al.* [FOCUS Collaboration], *Phys. Lett. B* **555** (2003) 167.
- [19] A. Bean *et al.* [CLEO Collaboration], *Phys. Lett. B* **317** (1993) 647.
- [20] K. Y. Gao *et al.* [CLEO Collaboration], arXiv:hep-ex/0408077, Submitted to the 32nd International Conference on High Energy Physics, August 2004, Beijing.